Binary Clusters AuPt and Au_6Pt: Structure and Reactivity within Density Functional Theory

Wei Quan Tian,*,†,‡ Maofa Ge,*,§ Fenglong Gu,⊥ Toshiki Yamada,|| and Yuriko Aoki‡,⊥

State Key Laboratory of Theoretical and Computational Chemistry, Institute of Theoretical chemistry, Jilin University, Changchun 130023, China, Department of Material Science, Faculty of Engineering Sciences, Kyushu University,6-1 Kasugakoen, Kasuga, Fukuoka, 816-8580, Japan, Institute of Chemistry, Chinese Academy of Sciences, Beijing 100080, P. R. China, Group, PRESTO, Japan Science and Technology Agency (JST), Kawaguchi Center Building, Honcho 4-1-8, Kawaguchi, Saitama, 332-0012, Japan, and Kansai Advanced Research Center, National Institute of Information and Communications Technology, 588−2 Iwaoka, Nishi-ku, Kobe 651-2492, Japan

Received: September 28, 2005; In Final Form: March 9, 2006

Within density functional theory with the general gradient approximation for the exchange and correlation, the bimetallic clusters AuPt and Au_6Pt have been studied for their structure and reactivity. The bond strength of AuPt lies between those of Au_2 and Pt_2, and it is closer to that of Au_2. The Pt atom is the reactive center in both AuPt and $AuPt^+$ according to electronic structure analysis. $AuPt^+$ is more stable than AuPt. Au_6Pt prefers electronic states with low multiplicity. The most stable conformation of Au_6Pt is a singlet and has quasi-planar hexagonal frame with Pt lying at the hexagonal center. The doping of Pt in Au cluster enhances the chemical regioselectivity of the Au cluster. The Pt atom essentially serves as electron donor and the Au atoms bonded to the Pt atom acts as electron acceptor in Au_6Pt. The lowest triplet of edge-capped rhombus Au_6Pt clusters is readily accessible with very small singlet−triplet energy gap (0.32 eV). O_2 prefers to adsorb on Au and CO prefers to adsorb on Pt. O_2 and CO have stronger adsorption on AuPt than they do on Au_6Pt. CO has a much stronger adsorption on AuPt bimetallic cluster than O_2 does. The adsorption of CO on Pt modifies the geometry of AuPt bimetallic clusters.

I. Introduction

Bimetallic clusters have drawn considerable attention in recent years due to their optical[1] and magnetic properties[2] and reactivities.[3] Some of the bimetallic clusters even have aromaticity.[4] In particular, bimetallic clusters and alloys are very attractive as catalysts with broad applications.[5] The interactions between the two components in bimetallic clusters introduce a mutual influence on the neighboring atoms and lead to unique properties for these clusters. The unique properties of bimetallic clusters, which originate from their unique electronic structure, consequently show different catalytic behaviors (e.g., catalytic selectivity) from those of the monometallic clusters.[6] The exploration of the structure of bare bimetallic clusters helps to understand the catalytic activity of the bimetallic catalyst and the interaction of the doped metal with the metal cluster.

The majority of studies on the binary transition metal clusters focus on their formation, structure,[7] and application in catalysis, magnetism, optics, thermodynamics, and mechanics.[1,2,5,8] Due to the multivalent bonding character and low-lying excited state, the geometric and electronic structures of most bimetallic clusters are complicated and remain to be elucidated. Among the transition bimetallic clusters, gold−platinum binary clusters attract strong attention for their potential application in catalysis.[3,6b,9] AuPt cluster shows different catalytic activity from that of pure Pt or Au clusters.[9a−c]

In present work, we study the structures of gold−platinum clusters AuPt and Au_6Pt within density functional theory (DFT).[10] Au_6Pt forms as the core in gold−platinum catalyst.[9a,9b] The studies on the structures and bonding between Pt and Au help to understand the unique catalytic activity of AuPt bimetallic clusters and the formation mechanism of bimetallic clusters.[9f,11] The different electronic configuration of gold ($5d^{10}6s^1$) and platinum ($5d^96s^1$) would differentiate the electronic structure of Au_6Pt from Au_7. Because of their similarity in structure, Au_6Pt and Au_7 can have some similar electronic properties. The relevant Au_7 clusters are also studied in the present work for comparison with Au_6Pt. The detailed structure and properties of Au_7 were investigated in ref 12. The possible ground state of Au_6Pt could be singlet or triplet since higher multiplicity for ground state of Pt and Pt_6Au clusters was predicted.[13] The transition from planar structure to a 3-dimensional structure for Au clusters occurs with 7 atoms.[13a,14] The doping of Pt may change the shape of the Au clusters. Recent studies[15] found the most stable structure of Au_6Pt is a planar hexagon with Pt lying at the center of the hexagon and concluded that the catalytic properties of the doped clusters are enhanced based on results of density of states analysis. However, we find this planar structure to be a transition state. Distortion of this structure results in a minimum, which is confirmed to be the most stable isomer for Au_6Pt in the present work.

Theoretical studies on adsorption of O_2[16] and CO[17] on small Au clusters found that O_2 binds very weakly to small Au clusters while CO has large adsorption energy on Au cluster.[17] Frontier

* Corresponding authors. E-mail: (W.Q.T.) wqtian@cube.kyushu-u.ac.jp; (M.G.) gemaofa@iccas.ac.cn.
† Jilin University.
‡ Kyushu University.
§ Chinese Academy of Sciences.
⊥ Japan Science and Technology Agency (JST).
|| National Institute of Information and Communications Technology.

10.1021/jp055506o CCC: $33.50 © 2006 American Chemical Society
Published on Web 04/21/2006

TABLE 1: Bond Distances (Å), Atomization Energies, Ionization Potentials (IP), Electron Affinities (EA) (eV), and Electronic Configurations of Au_2, Pt_2, AuPt, $AuPt^+$, and $AuPt^-$, Predicted at BPW91 with the LANL2DZ Basis Set and the LANL2 Pseudopotential[a]

	bond distance (Å)	atomization energy	IP	EA	electronic configuration
Au_2 (singlet)	2.551	2.04	9.55	−2.01	$5d^{9.94}6s^{1.04}6p^{0.02}$
Pt_2 (triplet)	2.386	3.29	9.39	−2.04	$5d^{8.92}6s^{1.07}6p^{0.01}$
AuPt (doublet)	2.511	2.30	9.41	−2.27	$Pt[5d^{8.86}6s^{1.16}6p^{0.01}]Au[5d^{9.90}6s^{1.06}6p^{0.01}]$
AuPt (quadruplet)	2.565	0.94			$Pt[5d^{9.12}6s^{1.05}6p^{0.01}]Au[5d^{9.70}6s^{1.06}6p^{0.04}]$
$AuPt^+$ (singlet)	2.666	2.33			$Pt[5d^{9.23}6s^{0.20}7p^{0.01}]Au[5d^{9.96}6s^{0.58}7p^{0.01}]$
$AuPt^+$ (triplet)	2.567	2.63			$Pt[5d^{8.68}6s^{0.78}6p^{0.02}]Au[5d^{9.80}6s^{0.71}6p^{0.02}]$
$AuPt^-$(singlet)	2.542	2.32			$Pt[5d^{9.62}6s^{1.03}6p^{0.02}7s^{0.01}]Au[5d^{9.89}6s^{1.40}6p^{0.04}7s^{0.01}]$
$AuPt^-$(triplet)	2.627	2.16			$Pt[5d^{9.00}6s^{1.52}6p^{0.01}7s^{0.01}]Au[5d^{9.79}6s^{1.61}6p^{0.02}7s^{0.01}]$

[a] All energies are calculated based on the electronic energy with zero point vibration energy correction. The experimental bond distance for Pt_2 is 2.333 Å,[30b] the experimental bonding energy and ionization potential for Pt_2 are 3.14 ± 0.02 eV and 8.68 ± 0.02 eV,[30a] respectively. The experimental bond distance and bonding energy for Au_2 are 2.473 Å and 2.306 ± 0.005 eV for Au_2,[31b] respectively.

molecular orbitals (FMOs) are very helpful to identify the adsorption site of small molecules on metal cluster surface.[18] We use FMOs to explore the chemical activity of AuPt and Au_6Pt clusters. We also compare the structural difference between Au_7 and Au_6Pt clusters. The chemical activity of AuPt and the most stable Au_6Pt isomer is further explored by single adsorption of O_2 or CO to find the site preference of adsorption and the effect of adsorption on structure of metal clusters.

II. Computational Method

DFT methods as implemented in Gaussian98 package[19] have been used for the calculations of structures and vibrational frequencies of Au_6Pt and Au_7. We use the generalized gradient approximation (GGA) of Becke[20] and Perdew[21] for exchange and correlation functional (BPW91). The success of BPW91 in predicting metal clusters has been proven in the studies of transition metal clusters.[8l,13b,22] Au has the largest relativistic effects,[23] which significantly affect the structure of small Au clusters.[13a] The relativistic effect also has substantial impact on the chemistry of 5d metal clusters.[24] As Au's neighbor, Pt also shows strong relativistic effects.[23] The relativistic 19-electron (18-electron for Pt) Los Alamos National Laboratory (LANL2DZ) effective core pseudopotentials[25] with the basis sets (3s3p2d) are employed in the present DFT studies partially accounting for the relativistic effects. 6-31G(d) basis set is applied to C and O. The spin−orbit coupling due to relativistic effect has negligible effect on the relative stability of Pt clusters though it increases the binding energy of Pt cluster.[26] Thus, neglecting spin−orbit coupling in the present work does not have a strong effect on the structural and relative stability prediction of Au_6Pt. No spin−orbit coupling is considered in the present work within the Kohn−Sham DFT scheme. The nature of stationary point on potential energy surface is verified by the second-order derivatives of the energy with respect to the atomic coordinates (Hessian) through vibrational frequency calculations. Natural bond orbital (NBO)[27] analysis is carried out on the most stable Au_6Pt structures and relevant Au_7 clusters for their electronic structures. Totally 21 minima have been located for Au_6Pt.

III. Results and Discussions

A. Pt_2 and Au_2. The geometric and electronic structures for Pt_2, Au_2, AuPt, $AuPt^+$, and $AuPt^-$ are listed in Table 1. The structures of Pt_2 and Au_2 have been studied in details in our previous quantum mechanic investigation[13b] and other theoretical works.[28,29] The experimental structures are also available for Pt_2[30] and Au_2.[31] Our DFT predictions of the bond distances, bonding energy, and ionization potential for Pt_2 and Au_2 are in good agreement with experiment. NBO analysis indicates that there is a single bond in Au_2 with sole contributions from 6s electrons. In triplet Pt_2, the Pt−Pt bond comprises hybridization of 6s (80%) and $5d_{z^2}$ (20%) natural atom orbital (Pt−Pt bond lies in the *z*-direction). In Au_2, the Au−Au σ single bond comprises 6s (95%) and $5d_{z^2}$ (5%). From the atomization energy as listed in Table 1, one can see that Pt−Pt bond of Pt_2 is shorter and much stronger than the Au−Au bond of Au_2. This is due to the stronger relativistic effect in Au[23] and more 5d orbitals participate in the bonding of Pt_2.

B. AuPt. AuPt was studied with multireference singles + double configuration interaction (MRSDCI), the ground state of AuPt was found to be $^2\Delta$ with bond distance 2.544 Å (2.574 Å with spin−orbital effects).[32] The ground state of $AuPt^+$ was predicted to be singlet $^1\Sigma^+$ with bond distance 2.600 Å (2.652 Å with spin−orbital effects) at MRSDCI level of theory.[32] The singlet of $AuPt^+$ is predicted to be 0.21 eV (0.36 eV with spin−orbital effects) more stable than the triplet ($^3\Delta$) in this work. With spin−orbital effects considered, the ground state of $AuPt^+$ was predicted to have multiconfiguration character.[32]

The bond distance of doublet AuPt predicted by GGA as shown in Table 1 is shorter than that from MRSDCI.[31] This is in the same trend for the Pt_2 bond distance predicted from GGA[13b] and CASSCF;[28a] i.e., GGA predicts a shorter bond distance that is closer to experiment for Pt_2. The bond in AuPt is a single σ bond with 48% Au[$5d_{z^2}$(7%) + 6s(93%)] and 52% Pt [$5d_{z^2}$(16%) + 6s(83%)] in α spin and 51% Au[$5d_{z^2}$(7%) + 6s(93%)] and 49% Pt[$5d_{z^2}$(14%) + 6s(86%)] in β spin according to the NBO analysis. The bond strength of AuPt (2.30 eV) lies between those of Pt_2 (3.29 eV) and Au_2 (2.04 eV), but it is closer to that of Au_2. The AuPt bond distance (2.511 Å) also lies between the bond distances of Pt_2 (2.386 Å) and Au_2 (2.551 Å) and it is closer to that of Au_2. Because of the singly occupied α highest occupied molecular orbital (HOMO) with main contribution from Pt $5d_{z^2}$ orbital in AuPt as shown in Figure 1, Pt is the reactive center as electron donor in chemical reaction. Quadruplet AuPt has slightly longer Pt−Au bond distance and much weaker bond strength than that of doublet AuPt; the atomization energy of quadruplet AuPt is 1.36 eV less than that of doublet AuPt.

Removal of one electron from AuPt results in $AuPt^+$. This cation is an isoelectronic structure to Pt_2. Within GGA, the ground state of $AuPt^+$ is a triplet. Triplet $AuPt^+$ is 0.30 eV more stable than singlet $AuPt^+$. Such small triplet−singlet split energy makes the mixing of configurations in the ground state of $AuPt^+$ possible. On the other hand, the triplet−singlet split energy of Pt_2 is larger (1.46 eV).[13b] The removal of an electron from AuPt results in the relocation of bonding and charge distribution in $AuPt^+$. In singlet $AuPt^+$, the net charge on Pt is 0.55. The Pt−Au bond in singlet $AuPt^+$ has major contribution from 72% Pt[$5d_{z^2}$(86%) + 6s(13%) + $6p_z$(1%)] and minor

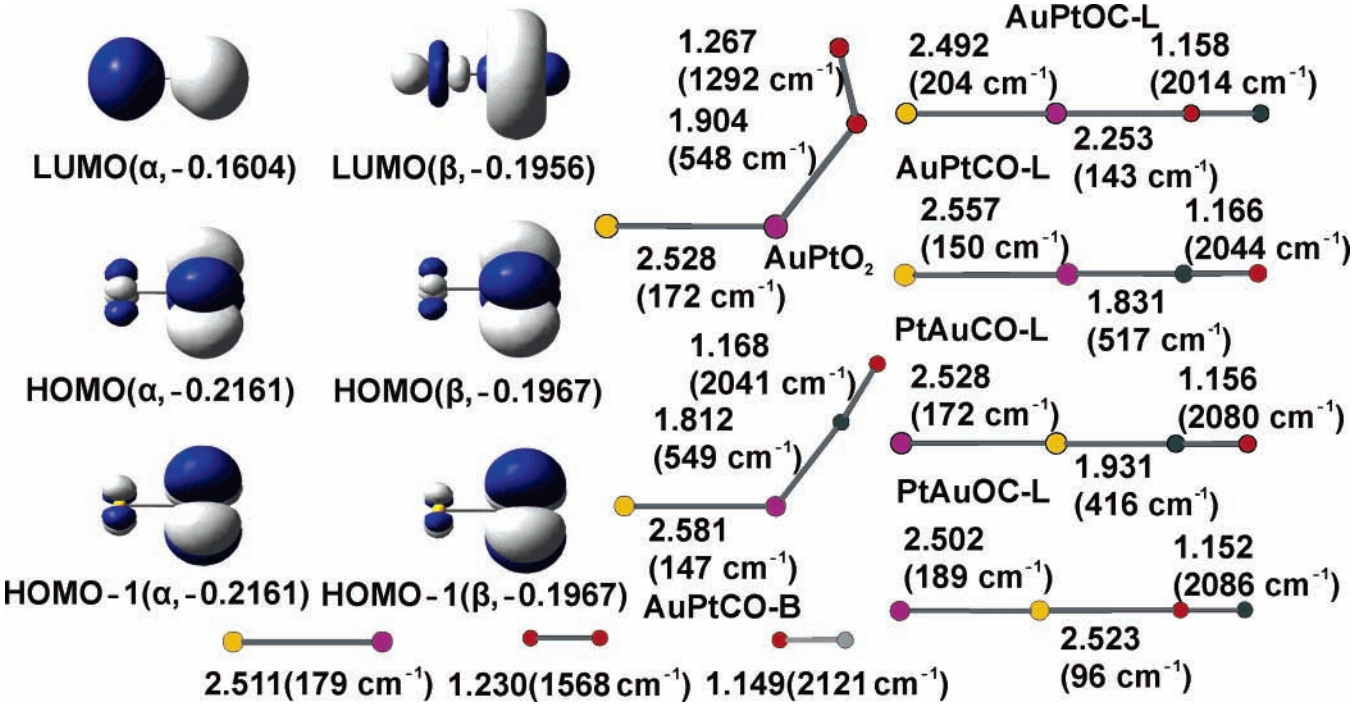

Figure 1. Structure, frontier molecular orbitals of AuPt, and adsorption of O_2 or CO on AuPt. The number outside of the parentheses is bond distances in angstrom between C and O or between Pt and C. The number in parentheses is the wavenumber of CO or PtC stretching vibrational frequency. The red atom is O. The gray (or black) atom is C. The purple atom is Pt. The yellow atom is Au.

contribution from 28% Au[$5d_{z^2}$(2%) + 6s(96%) + $6p_z$(2%)]; it is a single σ bond with Au 6s bonding with Pt $5d_{z^2}$. The $5d_{z^2}$ on Pt is empty. From the electronic structure of singlet $AuPt^+$, one can infer that an electron donor attacks Pt (due to the empty $5d_{z^2}$ orbital in the β LUMO) in a chemical reaction with singlet $AuPt^+$. In the triplet $AuPt^+$, an electron from $5d_{x^2-y^2}$ of Pt migrates to $5d_{z^2}$ to have an unpaired electron in each orbital. The net charge on Pt is 0.53 and the interatomic charge transfer (0.04) is from Pt to Au according to the electronic configuration of triplet $AuPt^+$ and the net charge on each atom. The bonding in triplet $AuPt^+$ changes accordingly. There are three one-electron bonds according to the composites of the bond. The nature of the first bond is 42% Au[$5d_{z^2}$(3%) + 6s(95%) + $6p_z$(2%)] with 58% Pt[$5d_{z^2}$(8%) + $6p_z$(1%) + 6s(90%)] in α spin; it is an s−s σ bond. The second one is 28% Au[$5d_{z^2}$(1%) + 6s(97%) + $6p_z$(2%)] with 72% Pt[$5d_{z^2}$(52%) − $5d_{x^2-y^2}$(25%) + 6s(23%)] in β spin; this bond is an Au(s)−Pt(∼d^4s) σ bond with a major contribution from Pt. The third one is 83% Au-[$5d_{z^2}$(91%) + $5d_{x^2-y^2}$(9%)] with 17% Pt[$5d_{z^2}$(25%) + $5d_{x^2-y^2}$(63%) + 6s(2%)] in β spin; it is a d−d polar σ bond with the main contribution from Au. The strong bond in triplet $AuPt^+$ renders triplet $AuPt^+$ larger atomization energy[33] than that of neutral AuPt and singlet $AuPt^+$ as listed in Table 1, i.e., triplet $AuPt^+$ has the strongest Au−Pt bond. The longer bond distance of triplet $AuPt^+$ (compared to AuPt) is the balance of the repulsion of the positive charges on Au and Pt, the decrease of s bonding contribution, and increase of d_{z^2} bonding contribution. The strong bonding in triplet $AuPt^+$ ensures that triplet is the ground state of $AuPt^+$.

The extra electron in singlet $AuPt^-$ mainly (0.68) goes to Pt $5d_{z^2}$ ($AuPt^-$ lies on the z axis), the rest goes to Au 6s atomic orbital. There is a σ bond with contributions from 65% Au-[$5d_{z^2}$(15%) + 6s((85%)] and 35% Pt[$5d_{z^2}$(25%) + 6s(75%)] in singlet $AuPt^-$, this bond is essentially an s−s σ bond. According to the electronic configuration of the triplet $AuPt^-$ as listed in Table 1, the triplet $AuPt^-$ is clearly an excited state and it is 0.16 eV above the singlet $AuPt^-$. From the atomization energy and bond distances, one notes that doublet AuPt, triplet $AuPt^+$ and singlet $AuPt^-$ are ground states. The ionization potential (IP) of AuPt lies between those of Au_2 and Pt_2, and it is mainly the 6s electron on Pt and Au removed from AuPt to form $AuPt^+$. The electron affinity of AuPt is larger than that of Au_2 and Pt_2, which is due to the strong electron accepting capacity of Pt 5d orbital as indicated by the electronic configurations of the doublet AuPt.

With the aid of NBO analysis, the electronic structure and bonding of AuPt and $AuPt^+$ are clearly revealed. This helps to understand the catalytic mechanism of AuPt and $AuPt^+$ in chemical reactions. AuPt and $AuPt^+$ will have different catalytic roles in catalyzed reactions according to their different electronic structures. They are also different from both Au_2 and Pt_2 as revealed in experiment.[3d,9f]

C. Adsorption of O_2 or CO on AuPt. To further check the chemical activity of AuPt, the adsorption of single O_2 or CO on AuPt is explored. The FMOs of AuPt, the bond distances, and major bond stretching frequencies of AuPt, O_2, CO, and O_2 or CO adsorbed AuPt are shown in Figure 1. The α lowest unoccupied molecular orbital (LUMO) is the σ* bond formed from the 6s atomic orbitals of Au and Pt. The β LUMO is the σ* bond formed from the $5d_{z^2}$ atomic orbitals of Au and Pt with major contribution from Pt and it is nearly degenerate with the β HOMO. The α HOMO is degenerate with the α occupied molecular orbital (MO) below it (HOMO-1). This is the same case for the β HOMO and β HOMO-1. The β HOMO has higher MO energy than the α HOMO, while the β LUMO has lower MO energy than the α LUMO. In chemical reaction, Pt is the active center according to the FMOs, though Au still can accept electron in the α LUMO.

Indeed, we locate only one minimum for O_2 adsorbed on AuPt at Pt ($AuPtO_2$ in Figure 1). $AuPtO_2$ has 3-dimensional structure with a dihedral angle 48.8°, which is the result of the interaction between the π* orbital of O_2 and the 5d orbitals of Pt. The adsorption of O_2 on AuPt produces 24.9 kcal/mol heat of formation, thus adsorption of O_2 on AuPt is much stronger than

TABLE 2: Adsorption Energy of O_2 or CO on AuPt Predicted Using BPW91 with LANL2 Relativistic Pseudopotentials and LANL2DZ Basis Set on Metals and 6-31G(d) on C and O[a]

isomer	ΔE (kcal/mol)	isomer	ΔE (kcal/mol)
AuPt−O_2	−24.9	AuPtCO−L	−56.0
AuPtCO−B	−57.2	PtAuCO−L	−32.6
AuPtOC−L	−4.2	PtAuOC−L	−1.5

[a] The negative sign means that the energy of the adsorbed product is lower than the separate reactants.

it does on Au_2.[16] According to the bond distance (1.904 Å) between Pt and O and the wavenumber (548 cm^{-1}) of the PtO bond stretching, the adsorption of O_2 on AuPt is chemical adsorption. The OO bond lengthens from 1.230 Å in gas phase to 1.267 Å in the adsorbed $AuPtO_2$. On the other hand, the AuPt interaction is hardly affected since only antibonding (or nonbonding since Au has very little contribution) MOs from AuPt involve in the adsorption, which is revealed by the AuPt bond distance and bond stretching as shown in Figure 1. The adsorption of O_2 on AuPt indicates the enhanced reactivity of AuPt binary clusters with respect to pure Au_2 cluster.

Five minima are located for adsorption of CO on AuPt, one with bent and planar structure and the other four are linear as shown in Figure 1. The adsorption energies of these minima are listed in Table 2. The most stable adsorbed AuPtCO structure is a bent one (AuPtCO−B in Figure 1) with C attacking Pt. The AuPtC angle is 127.8° and the PtCO angle is 173.7° in AuPtCO−B. Overall, adsorption of CO with C bonding to Pt or Au is much more energetically favorable than adsorption of CO with O bonding to Pt or Au as manifested by the adsorption energies as listed in Table 2. The PtO bond distance in CO adsorption on AuPt with O as bonding site (2.253 Å in AuPtOC−L in Figure 1) is much longer than the PtO bond distance (1.904 Å) in $AuPtO_2$. The AuPt bond distance in the CO adsorbed AuPt with O as the attacking atom is even shorter than the gas-phase AuPt bond distance, e.g. in AuPtOC−L and PtAuOC−L as shown in Figure 1. Thus, the adsorption of CO on AuPt with O as the attack atom stabilizes the AuPt bond. However, the much more favorable adsorption of CO on AuPt with C as attacking atom excludes the possibility with O as attacking atom. This is very clearly revealed by the FMOs of AuPt. The dominant contribution to the FMOs of AuPt from Pt ensures Pt as active center. CO can donate its HOMO σ electrons and accept electron to its π^* molecular orbitals when interacting with AuPt. The FMO analysis of AuPt toward adsorption of CO further corroborates the proposal using FMO as indication for adsorption preference of metal clusters.[18]

D. Structures of Au_7 and Au_6Pt. Before performing detailed analysis on the structures of Au_6Pt clusters, knowledge about the relevant Au_7 structures would help one to better understand the structure and properties of Au_6Pt clusters. There are 11 conformations for Au_7 located with the LANL2DZ pseudopotential Gaussian calculations[13b] (for comparison, only the Au_7 structures relevant to Au_6Pt are shown in Figure 1S). Doublet edge-capped rhombus (ECR) was found to be the most stable structure of Au_7 and its electronic structure was reported in our previous work.[13b] Six Au_6Pt minima form from substitution of one Au atom with Pt at different positions in the Au_7 ECR as shown in Figure 2. They are ECR1 in singlet and triplet, ECR2 in singlet and triplet, ECR3, and ECR4 in triplet. Only substitution of an Au atom by a Pt atom in ECR, edge-capped tetrahedron (ECT), hexagon (Hex), tricapped tetrahedron (TCT),

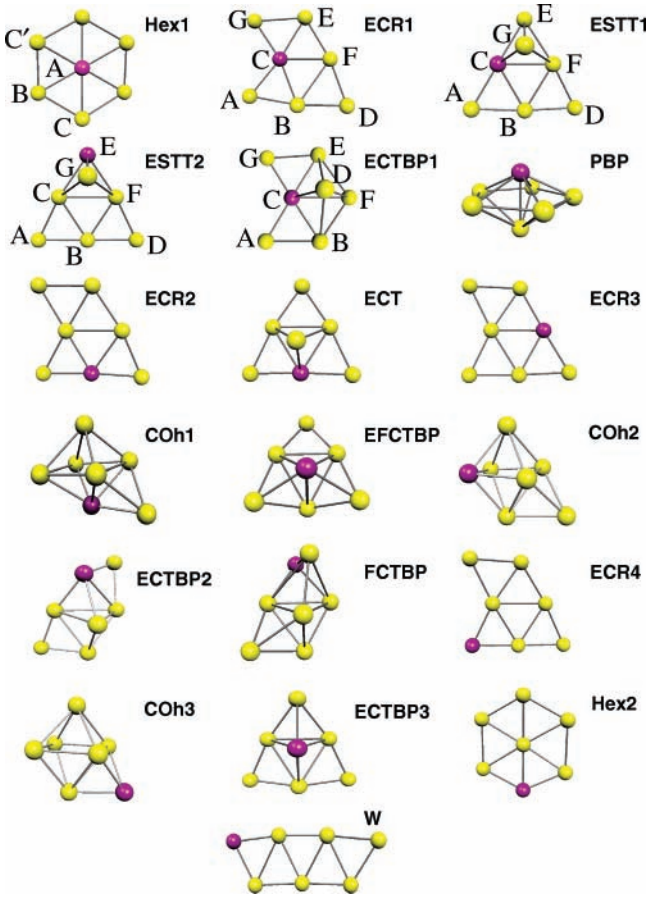

Figure 2. Structures of Au_6Pt clusters. The purple atom is Pt.

pentagonal bipyramid (PBP), capped "octahedron" (COh), and W Au_7 produces stable Au_6Pt conformations as shown in Figure 2.[34]

A total of 19 stable isomers with a total of 21 electronic states for Au_6Pt clusters have been located on the potential energy surface as shown in Figure 2. The relative energies of the 21 minima are listed in Table 3. The most stable conformation of Au_6Pt is predicted to be a closed-shell singlet hexagon (Hex) with Pt lying at the center of the hexagon (Hex1 in Figure 2). Analogous to Au_7, Au_6Pt prefers low multiplicity and a planar structure. In the first three most stable conformations (Hex1, ECR1, and edge-shared trapezoid and tetrahedron [ESTT or ESTT1]), Pt has maximum bonding with Au atoms. The most stable conformations are singlet ones, and a total of 7 minima have been located in singlet electronic state. Among the 14 conformations in triplet, ECR1 in (as shown in Figure 2) triplet is found to be the most stable conformation in triplet electronic state. It is 0.52 eV above the ground-state structure, singlet ECR1. We carry out detailed analysis on the electronic structure for the most stable conformations Hex1and ECR1 and the lowest triplet conformation ECR1 as well. The calculated first IP and EA as listed in Table 3 provide valuable information in comparison with experimental vertical detachment energies (VDE) and EA. In the following, we concentrate on an analysis of the structure of Au_6Pt Hex1 and Au_7 hexagon as well.

D.1. Hex1 Au_6Pt. The doublet Au_7 hexagon is analyzed in the present work for comparison with Au_6Pt Hex1. The FMOs, net spin, and natural atomic charges of doublet Au_7 hexagon and Hex Au_6Pt are shown in Figure 3. The Au_7 Hex has D_{2h} symmetry due to distortion from D_{6h} symmetry.[35] Due to the equivalence of the six surrounding Au atoms, these Au atoms have the same atomic structure and chemical activity. The net

TABLE 3: Relative Stability, Ionization Potential (IP) and Electron Affinity (EA) of Neutral Au_6Pt Bimetallic Heptamers Predicted Using BPW91 with LANL2 Relativistic Pseudopotentials and LANL2DZ Basis Set[a]

isomer	multiplicity	ΔE	IP	EA	isomer	multiplicity	ΔE	IP	EA
Hex1	1	0.00	7.91	−2.52	COh1	3	1.23	7.29	−3.07
ECR1	1	0.47	7.61	−3.01	EFCTBP	3	1.34	6.95	−3.17
ESTT1	1	0.51	7.34	−2.68	COh2	3	1.35	7.38	−3.02
ESTT2	1	0.52	7.75	−2.55	ECTBP2	3	1.37	7.32	−3.31
ECTBP1	1	0.59	7.52	−2.69	FCTBP	3	1.43	7.32	−3.14
PBP	1	0.74	7.59	−3.53	ECR4	3	1.51	7.20	−3.67
ECR2	1	0.84	7.54	−3.27	COh3	3	1.54	7.55	−3.23
ECR1	3	0.99	7.11	−3.56	ECTBP3	3	1.56	6.92	−3.46
ECR2	3	1.12	7.25	−3.63	Hex2	3	1.69	7.32	−2.75
ECT	3	1.17	7.78	−2.76	W	3	2.13	7.45	−3.62
ECR3	3	1.23	7.26	−3.37					

[a] All energies are in eV. EFCT: edge and face capped triangonal bipyramid. FCTBP: face capped triangonal bipyramid.

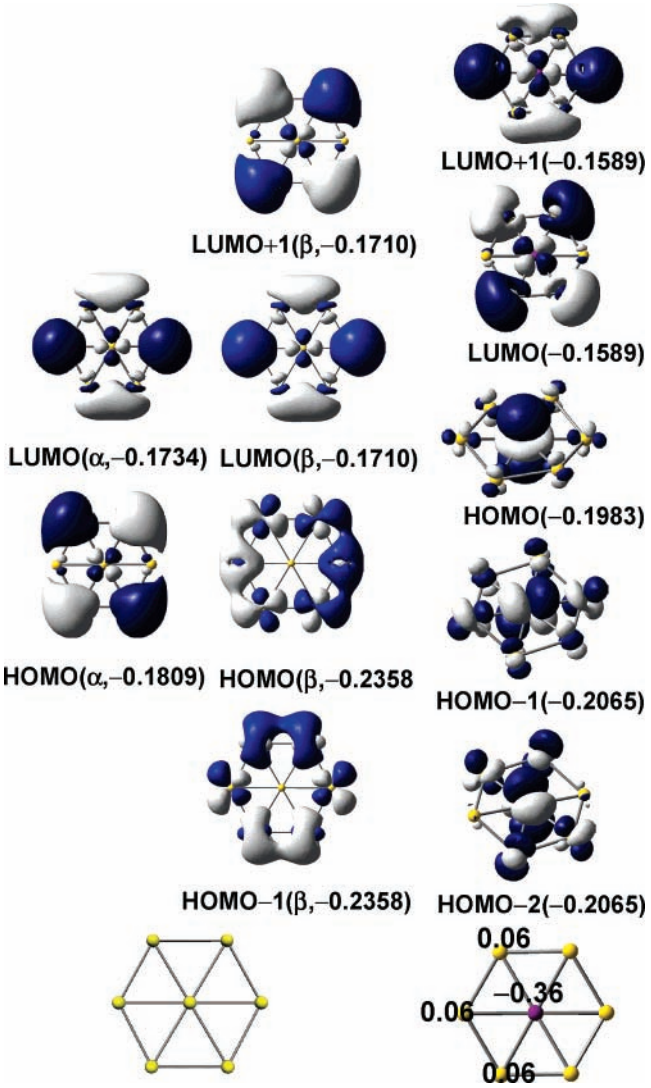

Figure 3. Frontier molecular orbitals and natural atomic charges (spin) of Hexgonal doublet Au_7 and singlet Au_6Pt predicted using BPW91 exchange-correlation functionals with LANL2DZ relativistic pseudopotential and Gaussian basis set. The number in the frontier molecular orbital lable is the orbital energy in a.u. The number on the structure is the natural atomic charge.

spin distributes among the six surrounding Au atoms equally. The HOMO(α)−LUMO(α) gap of the Au_7 Hex is 0.20 eV. The energy gap between the HOMO and the HOMO-1 (the occupied MO right below HOMO) for α spin is 1.57 eV (the two counterpart molecular orbtials of β spin are degenerate). The α spin energy gap between HOMO and HOMO-1 is mainly due to the 5d−6s Au atomic orbital gap, whereas for the β spin the

TABLE 4: Electronic Configurations of the Most Stable Minima of Au_6Pt Bimetallic Clusters[a]

atom	hex1 Au_6Pt
A	$Pt[5d^{9.39}6s^{0.85}6p^{0.09}6d^{0.02}]$
B	$Au[5d^{9.91}6s^{1.007}p^{0.02}]$

atom	ECR1 Au_6Pt	ECR1 Au_6Pt (triplet)
A	$Au[5d^{9.83}6s^{1.14}7p^{0.01}]$	$Au[5d^{9.83}6s^{1.14}6p^{0.01}]$
B	$Au[5d^{9.82}6s^{1.00}6p^{0.04}6d^{0.01}7p^{0.01}]$	$Au[5d^{9.87}6s^{0.98}6p^{0.04}7p^{0.01}]$
C	$Pt[5d^{9.35}6s^{0.91}6p^{0.06}6d^{0.02}]$	$Pt[5d^{9.16}6s^{0.88}6p^{0.07}6d^{0.02}]$
D	$Au[5d^{9.90}6s^{1.10}7p^{0.01}]$	$Au[5d^{9.88}6s^{1.20}6p^{0.01}]$
E	$Au[5d^{9.87}6s^{1.04}6p^{0.01}7p^{0.02}]$	$Au[5d^{9.83}6s^{1.05}6p^{0.03}]$
F	$Au[5d^{9.88}6s^{1.02}6p^{0.03}6d^{0.01}7p^{0.01}]$	$Au[5d^{9.84}6s^{1.06}6p^{0.04}7p^{0.01}]$
G	$Au[5d^{9.89}6s^{1.01}7p^{0.01}]$	$Au[5d^{9.83}6s^{1.20}6p^{0.01}]$

[a] The core electrons are not shown. The labels of atoms in each structure are shown in Figure 2. The electronic state of all conformations is singlet unless specified.

two molecular orbitals consist of 5d Au atomic orbitals in Hex Au_7. In chemical reaction, the six surrounding Au atoms are the active centers during the Au_7 Hex reacting with electron acceptor. Substitution of one Au atom in different positions in the Au_7 Hex results in two minima, Hex1 in singlet and Hex2 in triplet as shown in Figure 2.

Hex1 is at least 0.4 eV more stable than the second most stable conformation ECR1. Hex1 (in Figure 2) is a distorted hexagon structure with D_{3d} symmetry (for electronic structure) from D_{6h}[36] due to the degeneracy of the HOMO and the HOMO-1. The Pt atom lies at the center of the distorted hexagon and the distortion is slight. The C′ABC dihedral angle is 165.4°. The Au−Au bond distance is 2.74 Å and the Au−Pt bond distance is 2.72 Å in Hex1. Among all the located minima, Hex1 has the most bonding for Pt to Au in which Pt bonds to all the six Au atoms. The FMOs of Au_7 Hex and Au_6Pt Hex1 are shown in Figure 3 for further analysis on the electronic structure of Hex1. Charge transfer occurs from Au to Pt in Au_6Pt Hex1. From the electronic configuration of Hex1 Au_6Pt as listed in Table 4, one can see that the charge transfer from Au to Pt takes place from the Au 5d (d_{xy} and $d_{x^2-y^2}$) orbitals to the Pt 5d orbital (d_{xy} and $d_{x^2-y^2}$, Hex1 roughly lies in the *xy* plane). This d−d charge transfer from Au to Pt is due to the stronger relativistic effect of Au in which the destabilization of d orbitals is stronger in Au than that in Pt.[23] Electron promotion occurs in Pt atom and it is from 6s to 5d and 6p (about 0.15 electron). The maximum bonding of Pt with Au atoms and charge transfer from Au atoms to Pt are the main contributions to the stability of Hex1. The Pt atom has maximum bonding in Au_6Pt ECTBP1, the obvious nonplanarity of the Au moiety destabilizes this isomer.[12]

The HOMO of Hex1 (as shown in Figure 3) has major contribution from Pt $5d_{z^2}$ orbital. The degenerate occupied

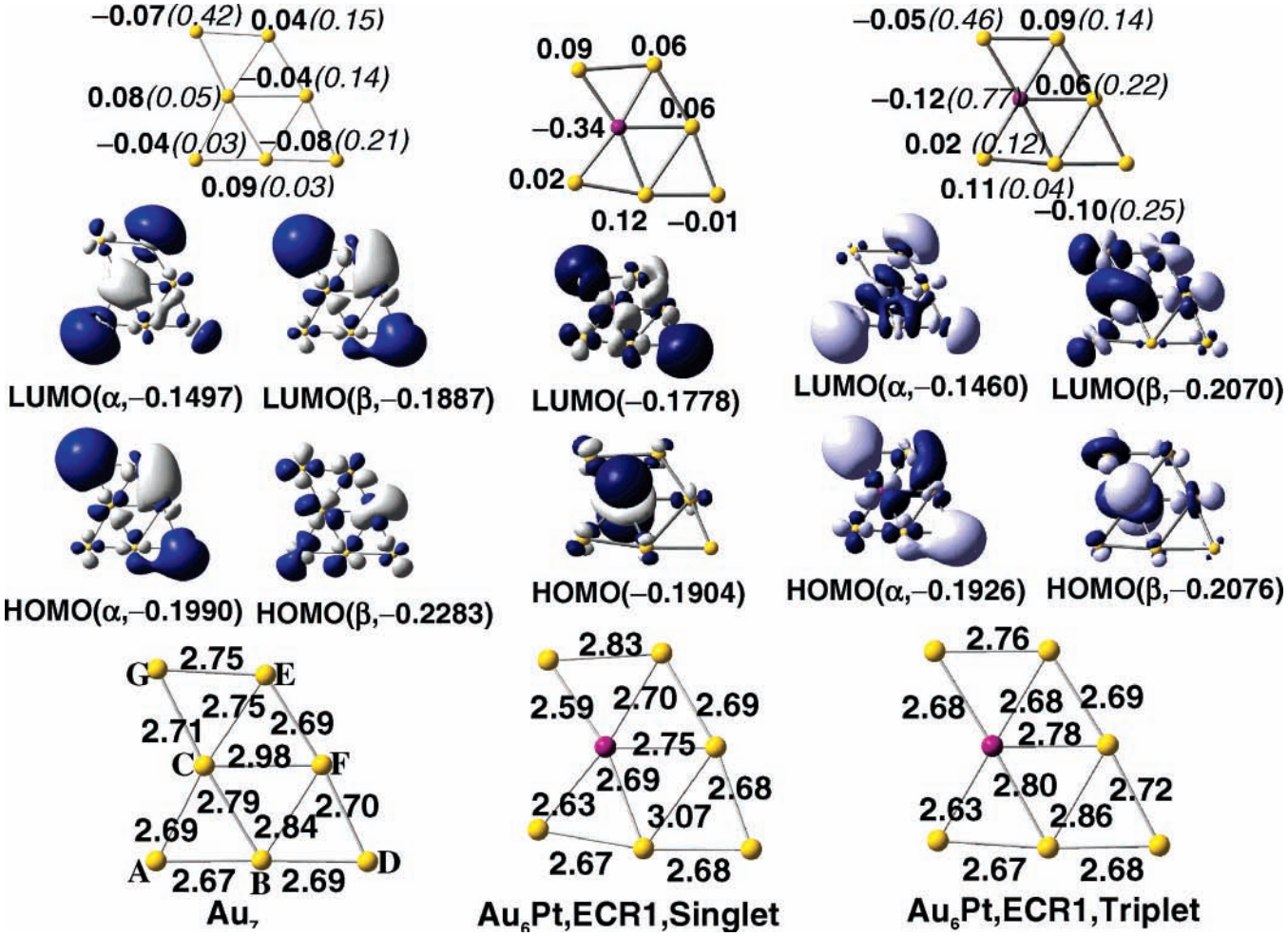

Figure 4. Frontier molecular orbitals and natural atomic charges (spin) of singlet and triplet ECR1 Au_6Pt predicted using BPW91 exchange-correlation functionals with LANL2DZ relativistic pseudopotential and Gaussian basis set. The number in the frontier molecular orbital label is the orbital energy in a.u. The number on the structure upper side outside of the parentheses is natural atomic charge and the number in the parentheses is atomic net spin. The number on the structure at lower side is bond distance in angstrom. The purple atom is Pt.

orbitals (the HOMO-1 and the HOMO-2) comprise the Pt $5d_{xz}$ and $5d_{yz}$ orbitals, respectively. The LUMO has dominant contribution from the surrounding Au atoms and it is degenerate with the LUMO-1. Because of the dominant contribution to the occupied FMOs from Pt, the doping of Pt significantly changes the chemical reactivity of gold cluster which renders the AuPt bimetallic clusters' unique chemistry. According to the HOMO and the LUMO of Hex1, the electron acceptor attacks Pt from below or above the Hex1 quasi-plane and electron donor attacks Au atoms within the Hex1 quasi-plane to have maximum MO overlap. The nearly degenerate low lying virtual MOs of Hex1 have exclusive contribution from the 6s Au atomic orbitals. This explains the IP and EA of Hex1 as listed in Table 3: the IP is mainly due to Pt, and the EA is mainly due to Au. In other words, the first electron removed from Hex1 resulting in Au_6Pt^+ is taken from the Pt atom and an extra electron goes to Au to form Au_6Pt^-. Since the EAs of Au clusters and Pt clusters are close,[28d] it is difficult to differentiate the contribution origins solely from the calculated values. The FMOs of the cluster facilitate the analysis of the origin of EA and IP in AuPt bimetallic clusters. The FMOs of Hex1 Au_6Pt also indicate the different chemical activity of Hex1 Au_6Pt. In Hex1 Au_6Pt^+, the active center is solely Pt since the singly occupied MO is on Pt. While in Hex1 Au_6Pt^-, the singly occupied MO is on Au atoms; thus, the active centers are Au atoms. This is clearly reflected by the FMOs of Hex1 Au_6Pt in Figure 3.

D.2. Singlet and Triplet ECR1 Au_6Pt. ECR1 can appear in metal cluster production due to kinetic reason. The Au_7 ECR was predicted to be the most stable conformation at the same level of theory.[13b] The structure of the Au_7 ECR is also compared with those of the Pt-doped ECR1 to obtain insights on the effect of doping on the electronic structure of metallic clusters. The bond distances of the Au_7 ECR, singlet, and triplet Au_6Pt ECR1, natural charge, net spin, and the FMOs of the three molecules are shown in Figure 4.

In the Au_7 ECR, atom C has net positive charge (0.08). Among the bonded Au atoms to C, atoms A, G, and F have net negative charges and atoms B and E have positive charges. According to the net spin, partial charges, and FMOs of ECR Au_7, atoms D, E, F, and G are active centers in chemical reaction. Both the HOMO and the LUMO in the Au_7 ECR have major contributions from Au 6s atomic orbitals and this indicates that the 6s Au orbitals accept or donate electrons in chemical reaction.

The substitution of Au at C position in Au_7 changes the electronic structure of the Au_7 ECR thus resulting in new chemical reactivity. The geometry of Au_6Pt ECR1 contracts due to the shortening of PtAu bonds. The most noticeable bond distance change is BF Au−Au bond. This bond lengthens 0.23 Å from the Au_7 ECR to the Au_6Pt ECR1 singlet. The lengthening of this bond is the consequence of the shortening of Pt−Au bonds with respect to their counterpart bonds in the

Au_7 ECR. All the Au atoms bonded to the Pt atom in the Au_6-Pt ECR1 donate electrons to Pt (mainly to Pt 5d atomic orbitals) resulting in net negative charges on Pt. The charge transfer from Au to Pt renders Pt as electron donor in reaction with the electron withdrawing reagent. This is confirmed by the HOMO of ECR1 as shown in Figure 4. The HOMO has dominant contribution from Pt $5d_{z^2}$ orbitals. It is likely that the electron acceptor attacks Pt from below or above ECR1 molecular plane and electron donor attacks G or D (preferably G) within the molecular plane.

The HOMO−LUMO gap (0.33 eV) in ECR1 singlet is so small that it can be readily excited to the lowest excited state. As listed in Table 3, the lowest triplet of ECR1 is just 0.52 eV above the singlet state. The singlet−triplet energy gap of another ECR conformation (ECR2 in Figure 2) is even smaller, and it is only 0.32 eV. Thus, it is necessary to study the electronic structure of the triplet ECR1 and compare its structure with that of the ECR1 singlet. The most significant geometric change in Au_6Pt ECR1 triplet from singlet Au_6Pt ECR1 is the Au−Au bond (BF): it shortens and gets close to that in Au_7 ECR. The overall structure of the Au_6Pt ECR1 triplet is closer to that of ECR Au_7 compared with that of the Au_6Pt ECR1 singlet.

The unpaired electrons mainly distribute on the Pt atom and the Au atom at position G in the Au_6Pt ECR1 triplet. The natural charges of these two atoms decrease with respect to those in the Au_6Pt ECR1 singlet. The Pt atom still has the largest negative charge, the Au atom at B has the largest positive charge. The noticeable change of the FMOs in triplet Au_6Pt ECR1 is that the α HOMO comprises Au 6s orbitals and the β LUMO has major contribution from the Pt 5d orbital. The β HOMO and LUMO are almost degenerate (ca. 0.02 eV); thus, the Pt atom can accept or donate electrons in the chemical reaction. The large net spin and negative charge on Au atoms D and G and their large contribution to the α HOMO render these two atoms chemical active centers: these two Au atoms serve as electron donors in reacting with an electron withdrawing reagent. According to the FMOs of the Au_6Pt ECR1 triplet, an extra electron will go to the Pt atom due to its large net spin and major contribution to the β LUMO. The reactivity of the Au_6Pt ECR1 triplet is different from that of the Au_6Pt ECR1 singlet. In the Au_6Pt ECR1 triplet, Pt acts as an electron acceptor, while it is an electron donor in the singlet Au_6Pt ECR1. In both electronic states, the Pt atom serves as the active center in the chemical reaction. Because of the small singlet−triplet energy gap, the reactivity of the Au_6Pt ECR1 would be due to a mixture of singlet and triplet and the singlet is very easy to be excited to the triplet.

Detailed electronic structure analysis on Au_6Pt Hex1 and singlet and triplet Au_6Pt ECR1 reveals that the doping of Pt in Au clusters indeed creates new active center in chemical reaction, thus broadening their application in catalytic industry.

E. Adsorption of O_2 or CO on Hex Au_6Pt. Only two minima are located for the adsorption of O_2 on Hex1 Au_6Pt as shown in Figure 5, one (Hex1-O_2) with O_2 bonding to Pt above the hexagon and the other one (Hex1-$O_2$1) with O_2 bonding to a Au atom on the edge of the hexagon. The adsorbed O_2 in Hex1-$O_2$1 cuts through the hexagon into two halves. Hex1-O_2 is 1.1 kcal/mol less stable than the separate reactants, while O_2 adsorption on Au stabilizes the product by 2.4 kcal/mol in Hex1-$O_2$1. The OO bond distance in Hex1-O_2 does not change much with respect to the isolated O_2. According to the OPt bond distance as shown in Figure 5, the adsorption of O_2 in Hex1-O_2 is physical adsorption. On the other hand, the adsorption of O_2 in Hex1-$O_2$1 has much shorter OAu bond distance and the

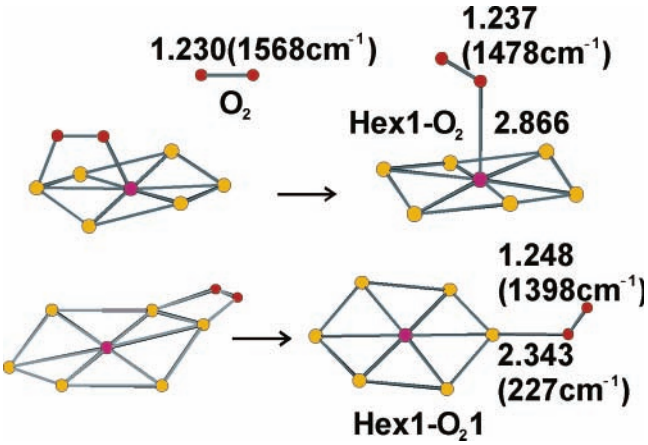

Figure 5. Adsorption of O_2 on Hex Au_6Pt. The number outside of the parentheses is bond distances in angstrom of O_2 or between Pt and O. The number in parentheses is the wavenumber of O_2 or PtO stretching vibrational frequency. The red atom is O. The purple atom is Pt. The yellow atom is Au.

TABLE 5: Adsorption Energy of O_2 or CO on Singlet Hex1 Au_6Pt Predicted Using BPW91 with LANL2 Relativistic Pseudopotentials and LANL2DZ Basis Set on Metals and 6-31G(d) on C and O

isomer	Δ*E* (kcal/mol)	isomer	Δ*E* (kcal/mol)
Hex-O_2	1.1	TCT-CO	−43.4
Hex-$O_2$1	−2.4	ESRT-CO	−25.8
EFCTBP−CO	−47.2	Hex1-CO	−24.9
PBP−CO	−44.5		

OO bond lengthens, thus O_2 has slightly stronger interaction with Hex1 Au_6Pt in Hex1-$O_2$1. The different interaction of O_2 with Hex1 Au_6Pt can be explained in term of FMOs of O_2 and Hex1 Au_6Pt. The antibonding π molecular orbitals of O_2 donates electrons to the LUMO of Hex1-O_2 while the contribution to the LUMO of Hex1-O_2 from Pt is very limited. Thus, this electron donation does not stabilize the complex though the electrostatic interaction between O_2 and Au_6Pt enhances the attraction between them. In Hex1-$O_2$1, the electrons in O_2 go to the LUMO of Au_6Pt, essentially to the 6s atomic orbitals of Au. The structure of Au_6Pt does not change much upon the adsorption of O_2, which further indicate the weak interaction between O_2 and Au_6Pt. The adsorption of O_2 on AuPt is much stronger than its adsorption on Au_6Pt.

Table 5 lists the adsorption energy of CO on Au_6Pt, and Figure 6 shows the structure, some critical bond distances, and wavenumber of bond stretching of CO adsorbed Hex1 Au_6Pt. In contrast to the adsorption of O_2 on Hex1 Au_6Pt, adsorption of CO on Hex1 Au_6Pt significantly changes the geometry of Hex1 Au_6Pt. A total of 5 minima are located for adsorption of CO on Hex1 Au_6Pt, among which 4 minima have nonplanar Au_6Pt. The only planar Au_6PtCO is Hex1-CO as shown in Figure 6. In Hex1-CO, C bonds to one Au atom with linear AuCO. This CO adsorption with C interacting with Au has similar bond distances at the adsorption site to those of PtAuCO-L as shown in Figure 1, though PtAuCO-L has larger adsorption energy. Another adsorbed minimum, edge-shared rhombus and tetrahedron Au_6Pt with CO (ESRT-CO), has CO with C interacting with Au. The C attached Au atom in ESRT-CO lies above the metal cluster plane and forms a linear AuCO structure. ESRT-CO is slightly more stable than Hex1-CO.

In all the C-bonded Hex1 Au_6Pt clusters, the hexagonal geometry distorts to three-dimensional structures as shown in Figure 6. The adsorption energies for all the adsorbed Hex1 Au_6Pt conformations are listed in Table 5. The adsorption energy

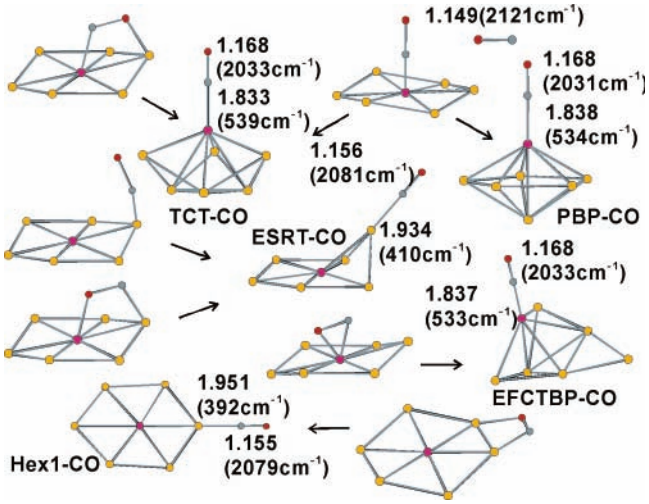

Figure 6. Adsorption of CO on Hex Au_6Pt. The number outside of parentheses is bond distances in angstrom between C and O, or between Pt and C. The number in parentheses is the wavenumber of CO or PtC stretching vibrational frequency. The red atom is O. The gray atom is C. The purple atom is Pt. The yellow atom is Au.

with Pt as adsorbing site is ca. 20 kcal/mol larger than that with Au as adsorbing site. The most stable CO adsorbed Au_6Pt from Hex1 Au_6Pt is PBP−CO with CO adsorbed on Pt and Pt is an apex of the PBP as shown in Figure 6. The adsorption of CO on Pt with C as attacking atom in Hex Au_6Pt is slightly weaker than its counterpart adsorption on AuPt according to the adsorption energy, PtC and CO bond distances, and the bond stretching frequency. According to the adsorption energy of CO on Au_6Pt, the adsorption with C as attacking atom is the preferred adsorption. The interaction of C end of CO with Pt drastically modifies the Au_6Pt cluster structure, which results from the strong forward electron donation from CO and backward electron donation from Pt to the antibonding π MOs of CO. The adsorption of CO on AuPt is much stronger than its adsorption on Au_6Pt. CO has much stronger adsorption on AuPt and Au_6Pt than O_2 does according to their adsorption energies. Our work reveals that Pt is indeed the active center of Pt doped Au cluster.[15]

IV. Conclusions

Within density functional theory, the most stable conformation for Au_6Pt is predicted to be a hexagon with Pt in the center with D_{3d} nuclear frame; its ground state is singlet. Au_6Pt clusters prefer singlet planar (or nearly planar) structure.

Charge transfer from Au to Pt occurs in Au_6Pt according to natural population analysis.

The doping of Pt in Au clusters certainly changes the electronic structure of Au clusters thus rendering new chemical reactivity; this is reflected in the frontier molecular orbitals of the binary clusters in which Pt 5d orbitals make a significant contribution.

The frontier occupied molecular orbitals of singlet Au_6Pt clusters have major contributions from Pt 5d atomic orbitals. In the nucleophile reaction, Pt serves as an electron donor.

The frontier virtual molecular orbitals of singlet Au_6Pt clusters mainly come from Au. In electrophile reaction, electrons will go to Au.

The new chemical reactivity of the Pt doped Au clusters are further verified by the adsorption of O_2 or CO on AuPt and hexagonal Au_6Pt: Pt is the preferred adsorption center and *C* is the attacking atom. The adsorption of CO is much stronger than the adsorption of O_2. The adsorption of O_2 and CO on AuPt is much stronger than their adsorption on Au_6Pt. The adsorption of CO with C as the attacking atom strongly distorts the hexagonal Au_6Pt structure.

According to the FMO analysis, the catalytic reaction would take place at the Pt atom probably with reaction mechanisms different from those of pure Au or Pt clusters. The exploration of the new catalytic properties of AuPt bimetallic clusters provides new insights into the catalytic selectivity of bimetallic clusters.

Note Added in Proof. During the review of this work, another work on the structure of Pt_mAu_n (however, only Pt_2Au_5 was studied for $m + n = 7$) and the CO adsorption on these clusters was published,[37] which supports the conclusion drawn in the present work that Pt is the active center.

Acknowledgment. W.Q.T. thanks the Japan Society for the Promotion of Science for a JSPS fellowship and Prof. Helmut Schwarz for the reprints of refs 3b, 9f, 9g, and 24. M.G. thanks the foundation of the Hundred Persons Talents. Y.A. and F.G. are grateful to the Research and Development Applying Advanced Computational Science and Technology of the Japan Science and Technology Agency (ACT-JST) and the Ministry of Education, Culture, Sports, Science, and Technology (MEXT) for financial support. We thank the reviewers for the critical comments.

Supporting Information Available: Figures showing structures of relevant Au_7, saddle points for Au_6Pt, density of states, partial density of states, and local density of states of the Hex1, ECR1 (singlet and triplet), ESTT1, ESTT2, and ECTBP1 Au_6Pt, a table of electronic configurations of ESTT1, ESTT2, and ECTBP1, figures showing infrared spectra of the Hex1Au_6Pt, singlet and triplet ECR1 Au_6Pt, and the adsorbed Au_6Pt minima, and tables giving the coordinates for all the Au_6Pt minima and the adsorbed Au_6Pt minima from Gaussian calculations. This material is available free of charge via the Internet at http://pubs.acs.org.

References and Notes

(1) (a) Link, S.; Wang, Z. L.; El-Sayed, M. A. *J. Phys. Chem. B* **1999**, *103*, 3529. (b) Zhang, H.; Zelmon, D. E.; Deng, L.; Liu, H.-K.; Teo, B. K. *J. Am. Chem. Soc.* **2001**, *123*, 11300. (c) Gaudry, M.; Lermé, J.; Cottancin, E.; Pellarin, M.; Vialle, J.-L.; Broyer, M.; Prével, B.; Treilleux, M.; Mélinon, P. *Phys. Rev. B* **2001**, *64*, 085407.

(2) (a) Stener, M.; Albert, K.; Rösch, N. *Inorg. Chim. Acta* **1999**, *286*, 30. (b) Bromley, S. T.; Catlow, C. R. A. *Int. J. Quantum Chem.* **2003**, *91*, 270.

(3) (a) Tada, H.; Suzuki, F.; Ito, S.; Akita, T.; Tanaka, K.; Kawahara, T.; Kobayashi, H. *J. Phys. Chem. B* **2002**, *106*, 8714. (b) Koszinowski, K.; Schröder, D.; Schwarz, H. *ChemPhysChem.* **2003**, *4*, 1233.

(4) (a) Li, X.; Kuznetsov, A. E.; Zhang, H.-F.; Boldyrev, A. I.; Wang, L.-S. *Science* **2001**, *291*, 859. (b) Seo, D.-K.; Corbett, J. D. *Science* **2001**, *291*, 841.

(5) (a) Sinfelt, J. H. *Bimetallic Catalysis: Discoveries, Concepts, and Applications*; Wiley: New York, 1983. (b) Hermans, S.; Raja, R.; Thomas, J. M.; Johnson, B. F. G.; Sankar, G.; Gleeson, D. *Angew. Chem., Int. Ed.* **2001**, *40*, 1211. (c) Gates, B. C.; Alexeev, O. S. *Ind. Eng. Chem. Res.* **2003**, *42*, 1571.

(6) (a) Bazin, D.; Mottet, C.; Tréglia, G. *Appl. Catal., A* **2000**, *200*, 47. (b) Mihut, C.; Descorme, C.; Duprez, D.; Amiridis, M. D. *J. Catal.* **2002**, *212*, 125. (c) Chandler, B. D.; Schabel, A. B.; Blandford, C. F.; Pignolet, L. H. *J. Catal.* **1999**, *187*, 367.

(7) (a) Harada, M.; Asakura, K.; Ueki, Y.; Toshima, N. *J. Phys. Chem.* **1993**, *97*, 10742. (b) Wang, H.; Carter, E. A. *J. Am. Chem. Soc.* **1993**, *115*, 2357. (c) Harada, M.; Asakura, K.; Toshima, N. *J. Phys. Chem.* **1994**, *98*, 2653. (b) López, M. J.; Marcos, P. A.; Alonso, J. A. *J. Chem. Phys.* **1996**, *104*, 1056. (d) Wagner, R. L.; Vann, W. D.; Castleman, A. W., Jr. *Rev. Sci. Instrum.* **1997**, *68*, 3010. (e) Casalis, L.; Günther, S.; Kovaè, J.; Marsi, M.; Kiskinova, M.; Bifone, A. *Chem. Phys. Lett.* **1998**, *290*, 245. (f) Malinowski, N.; Tast, F.; Branz, W.; Billas, I. M. L.; Martin, T. P. *J. Chem.*

Phys. **1999**, *110*, 9915. (g) Fortunelli, A.; Velasco, A. M. *J. Mol. Struct. THEOCHEM* **1999**, *487*, 251. (h) Rousset, J. L.; Cadete Santos Aires, F. J.; Sekhar, B. R.; Mélinon, P.; Prevel, B.; Pellarin, M. *J. Phys. Chem. B* **2000**, *104*, 5430. (i) Gaudry, M.; Lerme, J.; Cottancin, E.; Pellarin, M.; Vialle, J. L.; Broyer, M.; Prevel, B.; Treilleux, M.; Melinon, P. *Phys. Rev. B* **2001**, *64*, 085407. (j) Koyasu, K.; Mitsui, M.; Nakajima, A.; Kaya, K. *Chem. Phys. Lett.* **2002**, *358*, 224. (k) Darby, S.; Mortimer-Jones, T. V.; Johnston, R. L.; Roberts, C. *J. Chem. Phys.* **2002**, *116*, 1536. (l) Lee, H. M.; Ge, M.; Sahu, B. R.; Tarakeshwar, P.; Kim, K. S. *J. Phys. Chem. B* **2003**, *107*, 9994. (l) Weis, P.; Welz, O.; Vollmer, E.; Kappes, M. M. *J. Chem. Phys.* **2004**, *120*, 677.

(8) (a) Albert, K.; Neyman, K. M.; Pacchioni, G.; Rösch, N. *Inorg. Chem.* **1996**, *35*, 7370. (b) Diaz, G.; Garin, F.; Maire, G.; Alerasool, S.; Gonzalez, R. D. *Appl. Catal., A* **1995**, *124*, 33. (c) Hermann, P.; Simon, D.; Sautet, P.; Bigot, B. *J. Catal.* **1997**, *167*, 33. (d) Fortunelli, A.; Velasco, A. M. *J. Mol. Struct. THEOCHEM* **2000**, *528*, 1. (e) Dela Portilia, C.; Cruz, A.; Luna-García, H.; Poulain, E.; Bertin, V.; Castillo, S. *Int. J. Quantum Chem.* **2000**, *80*, 657. (f) Rousset, J. L.; Cdrot, A. M.; Cadets Santos Aires, F. J.; Renouprez, A.; Mélinon, P.; Perez, A.; Pellarin, M.; Vialle, J. L.; Broyer, M. *J. Chem. Phys.* **1995**, *102*, 8574. (g) Deivaraj, T. C.; Chen, W.; Lee, J. Y. *J. Mater. Chem.* **2003**, *13*, 2555.

(9) (a) Payne, N. C.; Ramachandran, R.; Schoettel, G.; Vittal, J. J.; Puddephatt, R. J. *Inorg. Chem.* **1991**, *30*, 4048. (b) Pignolet, L. H.; Aubart, M. A.; Craighead, K. L.; Gould, R. A. T.; Krogstad, D. A.; Wiley, J. S. *Coord. Chem. Rev.* **1995**, *143*, 219. (c) Yuan, Y.; Asakura, K.; Wan, H.; Tsai, K.; Iwasawa, Y. *J. Mol. Catal. A* **1997**, *122*, 147. (d) Chandler, B. D.; Schabel, A. B.; Pignolet, L. H. *J. Catal.* **2000**, *193*, 186. (e) Chandler, B. D.; Pignolet, L. H. *Catal. Today* **2001**, *65*, 39. (f) Koszinowski, K.; Schröder, D.; Schwarz, H. *Organometallics* **2004**, *23*, 1132. (g) Koszinowski, K.; Schröder, D.; Schwarz, H. *J. Am. Chem. Soc.* **2003**, *125*, 3676.

(10) (a) Hohenberg, P.; Kohn, W. *Phys. Rev.* **1964**, *136*, B864. (b) Kohn, W.; Sham, L. J. *Phys. Rev.* **1965**, *40*, A1133. (c) Parr, R. G.; Yang, W. *Density-functional theory of atoms and molecules*; Oxford University Press: New York, 1989.

(11) (a) Liz-Marzán, L. M.; Philipse, A. P. *J. Phys. Chem.* **1995**, *99*, 15120. (b) Remita, S.; Picq, G.; Khatouri, J.; Mostafavi, M. *Radiat. Phys. Chem.* **1999**, *54*, 463.

(12) (a) Häkkinen, H.; Landman, U. *Phys. Rev. B* **2000**, *62*, R2287. (b) Wang, J.; Wang, G.; Zhao, J. *Phys. Rev. B* **2002**, *66*, 035418. (b) Zhao, J.; Yang, J.; Hou, J. G. *Phys. Rev. B* **2003**, *67*, 085404. (c) Häkkinen, H.; Yoon, B.; Landman, U.; Li, X.; Zhai, H. J.; Wang, L. S. *J. Phys. Chem. A* **2003**, *107*, 6168.

(13) (a) Häkkinen, H.; Moseler, M.; Landman, U. *Phys. Rev. Lett.* **2002**, *89*, 033401. (b) Tian, W. Q.; Ge, M.; Sahu, B. R.; Wang, D. X.; Yamada, T.; Mashiko, S. *J. Phys. Chem. A* **2004**, *108*, 3806. (c) Tian, W. Q.; Ge, M.; Gu, F.; Aoki, Y. *J. Phys. Chem. A* **2005**, *109*, 9860.

(14) Olson, R. M.; Varganov, S.; Gordon, M. S.; Metiu, H.; Chretian, S.; Piecuch, P.; Kowalski, K.; Kucharski, S. A.; Musial, M. *J. Am. Chem. Soc.* **2005**, *127*, 1049.

(15) Yuan, D. W.; Wang, Y.; Zeng, Z. *J. Chem. Phys.* **2005**, *122*, 114310.

(16) (a) Varganov, S. A.; Olson, R. M.; Gordon, M. S. *J. Chem. Phys.* **2003**, *119*, 2531. (b) Mills, G.; Gordon, M. S.; Metiu, H. *Chem. Phys. Lett.* **2002**, *359*, 493.

(17) Mills, G.; Gordon, M. S.; Metiu, H. *J. Chem. Phys.* **2002**, *117*, 4010.

(18) (a) Chrétien, S.; Gordon, M. S.; Metiu, H. *J. Chem. Phys.* **2004**, *121*, 3756. (b) Chrétien, S.; Gordon, M. S.; Metiu, H. *J. Chem. Phys.* **2004**, *121*, 9926. (c) Chrétien, S.; Gordon, M. S.; Metiu, H. *J. Chem. Phys.* **2004**, *121*, 9931.

(19) Gaussian 98 (Revision A.7), Gaussian, Inc.: Pittsburgh, PA, 1998 (www.Gaussian.com).

(20) Becke, A. D. *Phys. Rev. A* **1988**, *38*, 3098.

(21) (a) Perdew, J. P.; Chevary, J. A.; Vosko, S. H.; Jackson, K. A.; Pederson, M. R.; Singh, D. J.; Fiolhais, C. *Phys. Rev. B* **1992**, *46*, 6671. (b) Perdew, J. P.; Burke, K.; Wang, Y. *Phys. Rev. B* **1996**, *54*, 16533.

(22) (a) Li, T.; Balbuena, P. B. *J. Phys. Chem. B* **2001**, *105*, 9943. (b) Wang, X.; Andrews, L. *J. Phys. Chem. A* **2001**, *105*, 5812. (c) Andrews, L.; Wang, X.; Manceron, L. *J. Chem. Phys.* **2001**, *114*, 1559.

(23) Pyykkö, P. *Chem. Rev.* **1988**, *88*, 563.

(24) Schwarz, H. *Angew. Chem., Int. Ed.* **2003**, *42*, 4442.

(25) Hay, P. J.; Wadt, W. R. *J. Chem. Phys.* **1985**, *82*, 299.

(26) Xiao, L.; Wang, L. *J. Phys. Chem. A* **2004**, *108*, 8605.

(27) Reed, A. E.; Curtiss, L. A.; Weinhold, F. *Chem. Rev.* **1988**, *88*, 899.

(28) (a) Balasubramanian, K. *J. Chem. Phys.* **1987**, *87*, 6573. (b) Harada, M.; Dexpert, H. *J. Phys. Chem.* **1996**, *100*, 565. (c) Varga, S.; Fricke, B.; Nakamatsu, H.; Mukoyama, T.; Anton, J.; Geschke, D.; Heitmann, A.; Engel, E.; Baştuğ, T. *J. Chem. Phys.* **2000**, *112*, 3499. (d) Grönbeck, H.; Andreoni, W. *Chem. Phys.* **2000**, *262*, 1.

(29) (a) Ortiz, G.; Ballone, P. *Phys. Rev. B* **1991**, *44*, 5881. (b) Hess, B. H.; Kaldor, U. *J. Chem. Phys.* **2000**, *112*, 1809. (c) Bonaèić-Koutecký, V.; Burda, J.; Mitrić, R.; Ge, M.; Zampella, G.; Fantucci, P. *J. Chem. Phys.* **2002**, *117*, 3120.

(30) (a) Taylor, S.; Lemire, G. W.; Hamrick, Y. M.; Fu, Z.; Morse, M. D. *J. Chem. Phys.* **1988**, *89*, 5517. (b) Marc, B. A.; Morse, M. D. *J. Chem. Phys.* **2002**, *116*, 1313.

(31) (a) Morse, M. D. *Chem. Rev.* **1986**, *86*, 1049. (b) Simard, B.; Hackett, P. A. *J. Mol. Spectrosc.* **1990**, *142*, 310. (c) James, A. M.; Kowalczyk, P.; Simard, B.; Pinegar, J. C.; Morse, M. D. *J. Mol. Spectrosc.* **1994**, *168*, 248.

(32) Dai, D.; Balasubramanian, K. *J. Chem. Phys.* **1994**, *100*, 4401.

(33) The atomization energy for $AuPt^+$ is calculated according to the electronic configuration with respect to the electronic configuration of Pt ($5d^96s^1$), $Pt^+(5d^9)$, Au($5d^{10}6s^1$), and $Au^+(5d^{10})$. For $AuPt^+$: $E(AuPt^+) = E(AuPt^+) - E(Au^+) - E(Pt)$. For $AuPt^-$: $E(AuPt^-) = E(AuPt^-) - E(Au) - E(Pt^-)$.

(34) There are many saddle points generated from the substitution. The structure and coordinates of the saddle points and the coordinates of the minima are listed in Supporting Information.

(35) The bond distances in Hex Au_7 are as follows (labels are shown in Figure 1S): A−B(B′), 2.72 Å; A−(C′), 2.81 Å; B(B′)−C(C′), 2.73 Å; C−C′, 2.86 Å. The distortion from D_{6h} to D_{2h} is probably due to the exchange of the degenerate β HOMO and HOMO-1 and uneven occupancy of the α (HOMO) and the β (LUMO+1) molecular orbitals comprising Au 6s atomic orbitals.

(36) The Au−Au and Au−Pt bond distances in the D_{6h} hexagonal Au_6-Pt are 2.73 Å. The dihedron angle $D_{CBAC'}$ in D_{3d} hexagonal Au_6Pt is 165.4°. The energy lowering from D_{6h} to D_{3d} hexagonal Au_6Pt is 0.024 kcal/mol.

(37) Song, C.; Ge, Q.; Wang, L. *J. Phys. Chem. B* **2005**, *109*, 22341.